COMPTES RENDUS

CHIMIE

Full paper / Mémoire

DFT study of furan adsorption over stable molybdenum sulfide catalyst under HDO conditions

Michael Badawi, Sylvain Cristol, Jean-François Paul*, Edmond Payen

Unité de catalyse et chimie du solide − UMR CNRS 8181, Université des sciences et technologies de Lille, bâtiment C3, 59655 Villeneuve d'Ascq cedex, France

Abstract

We present a theoretical study on the furan hydrodeoxygenation (HDO) catalyzed by MoS_2, which is a model molecule for biomass valorization into oil. The stability of the MoS_2 catalyst depends on the H_2S/H_2O ratio during the reaction. The metallic edge is stable whatever the value of this ratio. In contrast, a H_2S pressure must be kept to prevent the sulfur edge from a partial oxygenation. The furan cannot be adsorbed on the stable surface. However, once a vacancy has been created by removing a sulfur atom from the metallic edge, the adsorption through its oxygen atom (η_1) is possible. ***To cite this article: M. Badawi et al., C. R. Chimie 12 (2009).***

Résumé

Nous présentons une étude théorique sur l'hydrodésoxygénation (HDO) du furane, molécule modèle pour la valorisation de la biomasse en carburant, catalysée par MoS_2. La stabilité de ce catalyseur dépend du rapport H_2S/H_2O pendant la réaction. Le bord métallique est stable quelle que soit la valeur de ce rapport. En revanche, une pression en H_2S doit être maintenue afin d'éviter une oxygénation partielle du bord soufré. Le furane ne peut être adsorbé sur la surface stable. Cependant, une fois une lacune créée en retirant un atome de soufre du bord métallique, l'adsorption du furane par son atome d'oxygène (η_1) est possible. ***Pour citer cet article : M. Badawi et al., C. R. Chimie 12 (2009).***

1. Introduction

The increase in crude oil prices and desire to limit carbon dioxide emissions from fossil fuels implies the diversification of the sources of liquid fuels. In this context, the European Union has set an objective of substituting 20% of the conventional fuels with alternative fuels in the road transport sector by the year 2020 [1]. One possibility is to produce oil by pyrolysis of biomass such as wood waste, which is a renewable source. However, wood-derived bio-oil fractions

* Corresponding author.
   E-mail address: jean-francois.paul@univ-lille1.fr (J.-F. Paul).

resulting from this pyrolysis contain very important amounts (up to 45 wt%) of oxygenated compounds [2,3]. These molecules present multiple functions like aldehyde, ketone, acids, and alcohols. High oxygen content leads to deleterious properties such as high viscosity, thermal and chemical instability [3,4]. Therefore, upgrading of bio-oils by reducing their oxygen content is required to obtain a usable fuel. Hydrodeoxygenation (HDO), which occurs during hydroprocessing, refers to the high temperature hydrogen treatment of the feed to obtain oxygen-free molecules. Oxygen is then removed in the form of water. Sulfided hydrotreating catalysts such as CoMo/Al_2O_3 and NiMo/Al_2O_3 are commonly used in HDO [3−8]. These catalysts, which are massively used in hydrodesulfurization (HDS) and hydrodenitrogenation (HDN) processes have been investigated extensively [5,9−15].

It is now well accepted that active sites are located on the edges of MoS_2 nanocrystallites that correspond to the (100) edge plane of the layered structure [5]. This crystallographic (100) plane exhibits alternative rows of sulfur-terminated layers (hereafter called S, or sulfur edge) and molybdenum-terminated layers (hereafter called M, or molybdenum edge) [16,17]. Stability of the catalysts is crucial, as interaction of water and oxygen-containing compounds with the catalysts can modify the sulfide structure of the catalyst edges [3]. Unfortunately, the stability of sulfide phases in presence of water, under usual HDO conditions, is still unknown.

Furan, one of the simplest oxygenated molecules present in HDO fractions, has been used to evaluate the activity of different catalysts. The reaction products of furan hydrodeoxygenation are butane and different isomers of butene, but the question of the primary products (tetrahydrofuran or butadiene) is still a matter of controversy; some mechanisms have been proposed in the literature [3,6] but they remain unclear. Density functional theory (DFT) calculations may provide insight into the furan HDO mechanism but require a detailed study of the adsorption of this molecule on the active MoS_2 phase. A similar work concerning the thiophene adsorption [18], a typical model compound used in HDS studies, showed the importance of an accurate description of the surface taking into account the nature of the surrounding atmosphere [12−15,18]. Therefore, in a first step, the stable surfaces of the catalyst MoS_2 under usual HDO conditions are determined using periodic DFT calculations. Then furan adsorption geometries on the MoS_2 (100) surfaces are systematically investigated on surfaces stable under HDO catalytic conditions.

2. Computational methods

The density functional theory (DFT) calculations were performed with the Vienna Ab initio Simulation Package (VASP) [19,20] based on Mermin's finite temperature DFT [21]. The wavefunction is expanded in a plane wave basis set and the electron−ion interactions are described using the projector augmented plane wave (PAW) method [22,23]. The solution of the Kohn−Sham equations was improved self-consistently until a difference lower than 10^{-5} eV was obtained between successive iterations. The calculations were performed at the Γ point with a cut-off energy of 450 eV and a Methfessel and Paxton [24] smearing with $\sigma = 0.1$ eV. The exchange correlation functional of Perdew and Zunger [25] was used with the generalized gradient corrections proposed by Perdew et al. [26]. For more details about the code, we refer the reader to Ref. [19,20].

Throughout this work, we used the large super cell ($12.641 \times 12.294 \times 20.000$ Å^3) shown in Fig. 1, which contains four elementary MoS_2 units in the x direction, four in the z direction, and two layers along the y-axis (Fig. 1). Previous studies [12−15,17,27,28] showed that this model is suitable to predict the electronic and structural properties of the MoS_2 surface. A vacuum layer of 10 Å is located above the MoS_2 slab in the z direction in order to avoid interactions between slabs. The two upper rows were allowed to relax until forces acting on ions are smaller than 3.10^{-2} eV Å^{-1}. The two lower were kept fixed to simulate bulk constraints.

3. Surface stability in the presence of water

3.1. Reference surface

Under working conditions, the presence of H_2, H_2S and H_2O will modify the stoichiometry and the nature of the atoms on the edges of the catalyst active phase. Experimentally, the catalyst is first sulfided and kept under hydrogen pressure before the introduction of the feed containing oxygen compounds. Therefore the initial structure is only dependent on the H_2/H_2S partial pressure ratio. In reducing conditions, the most stable surface [27,28], which will be used as reference, is presented in Fig. 2. We then investigate sulfur−oxygen exchange reaction and various oxygen stoichiometries in order to determine the effect of water on the surface stability.

Under hydrotreating conditions, the molybdenum edge is covered with sulfur atoms (Fig. 2), yielding six-fold-coordinated Mo edge atoms [15,27,29]. The
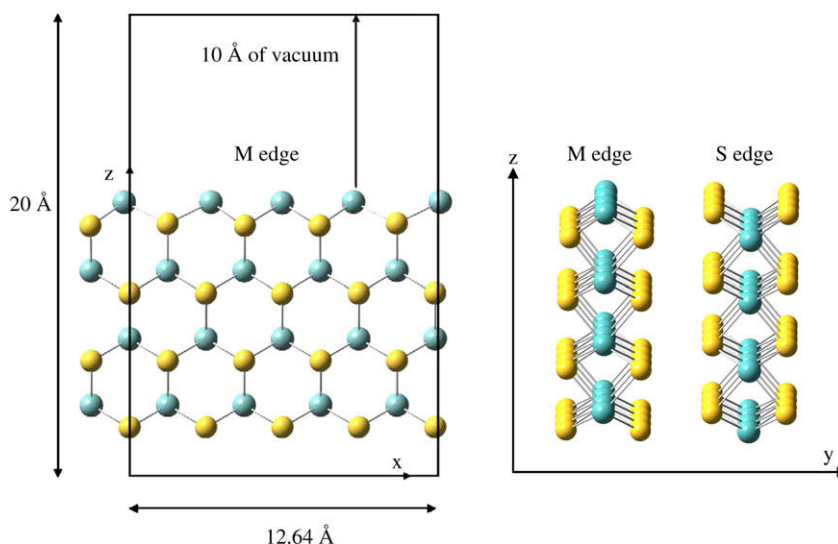
Fig. 1. Cell showing the perfect MoS$_2$ (100) surface. Molybdenum atoms are in blue, sulfur atoms are in yellow.

surface undergoes an important reconstruction with the formation of short (2.8 Å) and long (3.5 Å) Mo−Mo distances. Within the same partial pressure and temperature range, the sulfur edge is reduced: half of the sulfur atoms are removed from the surface leading to four-fold-coordinated molybdenum atoms.

3.2. Sulfur−oxygen exchange

Under hydrodeoxygenation conditions, a large amount of water is produced because of the very high content of oxygenated compounds in the feedstock [3]. These compounds and H$_2$O can depose oxygen atoms on the unsaturated molybdenum atoms and modify the surface state. Sulfur−oxygen exchanges can take place on the stable reference surface named hereafter surface [0-0] according to reaction (1).

$$\text{surface}[0 - 0] + n\text{H}_2\text{O} = \text{surface}[x - y] + n\text{H}_2\text{S} \qquad (1)$$
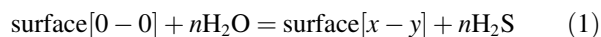
with x: number of oxygen atoms on the sulfur edge, y: number of oxygen atoms on the metallic edge

$$x + y = n$$

Taking water as the oxygen source, successive exchanges (up to $n = 6$) were studied on both edges. The calculated surfaces will be noted $[Z - y]$ or $[x - Z]$ to indicate that the treated edge carries x or y oxygen atoms, while the second one is undefined as we assumed that the interaction between the 2 edges is small and that the edges can be studied separately. The computed electronic energies of each surface are reported in Table 1.

Whatever the edge and the number of oxygen atom, the reaction is endothermic but the exchange will be favoured on the sulfur edge. Indeed, the energy required per S−O exchange for $n = 1 - 4$ is around 0.9 eV on the M-
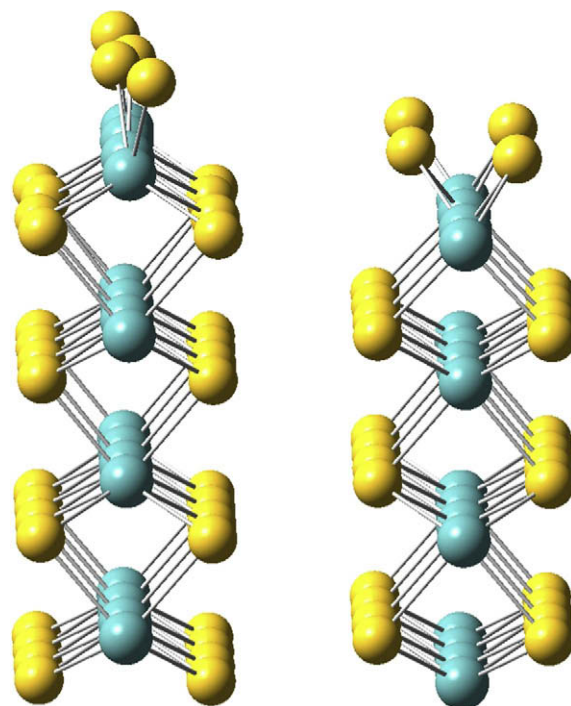

Fig. 2. MoS$_2$ stable surface when $0.05 < \text{H}_2\text{S}/\text{H}_2 < 10{,}000$ [23,24] that will be used as reference. The M-edge is on the left, the S-edge is on the right.

Table 1
Electronic contribution for the S—O exchange reaction from the reference surface [0-0].

	Surface	n	Energy required to perform the nth exchange (eV)	ΔE_n (eV)	Energy per exchanged oxygen atom $\Delta E_n/n$ (eV)
M-edge	[Z-1]	1	0.90	0.90	0.90
	[Z-2]	2	0.75	1.65	0.83
	[Z-3]	3	0.97	2.62	0.87
	[Z-4]	4	0.91	3.53	0.88
S-edge	[1-Z]	1	0.27	0.27	0.27
	[2-Z]	2	0.39	0.66	0.33
	[3-Z]	3	0.50	1.16	0.39
	[4-Z]	4	0.46	1.62	0.41
	[5-Z]	5	0.85	2.47	0.49
	[6-Z]	6	0.82	3.29	0.55

edge whereas it is around 0.4 eV on the S-edge (Table 1). On the metallic edge, the exchange energy is similar for the atom on the edge and for the neighboring atoms on the basal plane, and thus the exchange energy is almost constant for the substitution of the first 4 atoms. On the sulfur edge, the exchange energy for the substitution of one edge atom is 0.4 eV (for 1—4 exchange) while it is 0.9 eV for the substitution of the neighboring basal plane atoms. The average exchange energy will increase when all the 4 sulfur atoms on the edge have been substitute by oxygen ones.

3.3. Thermodynamic contributions

In order to define the most stable surfaces in the catalytic conditions, the S—O exchange reactions' Gibbs free energies are computed according to reaction (1):

$$\Delta_r G = \mu(\text{surface}[x-y]) - \mu(\text{surface}[0-0])$$
$$+ n(\mu(H_2S) - \mu(H_2O))$$

Assuming that the difference between the chemical potentials μ of solid phases can be approximated by the difference in their electronic energies, we can compute:

$$\Delta_r G = \Delta E_n + n\Delta\mu$$

where $\Delta E_n = E(\text{surface}\ [x-y]) - E(\text{surface}\ [0\text{-}0]) + nE(H_2S) - nE(H_2O)$ is the electronic contribution for the S—O exchange reaction, and $\Delta\mu = \Delta\mu^0(T) + R \times T \times \ln 10 \times \log((P(H_2S))/(P(H_2O)))$ is the difference between hydrogen sulfide and water chemical potentials.

$\Delta\mu^0(T) = \Delta ZPE + \Delta H_{vib} + \Delta H_{rot} + \Delta H_{tr} - T(\Delta S_{vib} + \Delta S_{rot} + \Delta S_{tr})$ is computed with the
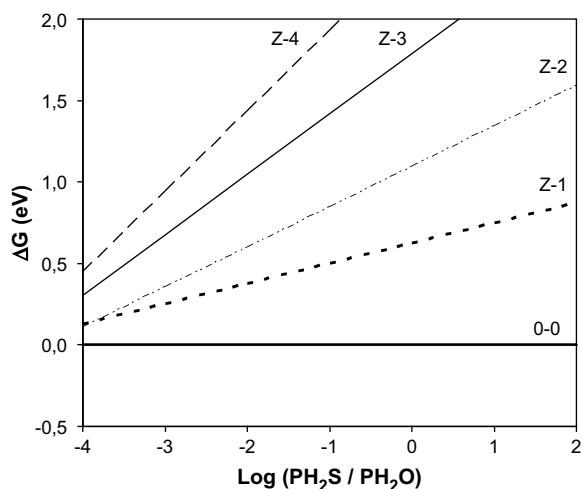

Fig. 3. Metallic edge: variation of the Gibbs free energy versus $\log((P(H_2S))/(P(H_2O)))$.

partition functions of each molecule using the standard formulas of statistical thermodynamics [30,31]. ΔZPE refers to zero point energy (due to the vibrations) between the molecules.

This equation leads to a linear relationship between $\Delta_r G$ and $\log((P(H_2S))/(P(H_2O)))$ that is represented for each surface in Fig. 3 (M-edge) and Fig. 4 (S-edge). The calculations were performed at $T = 350\ °C$, which corresponds to the working temperature of the catalyst and H_2S/H_2O partial pressure ratios between 10^{-4} and 100 $(0.0001 < H_2S/H_2O < 100)$. The most stable surface is obviously that presenting the lowest free energy that is represented on the diagrams by the lowest line for each $P(H_2S)/P(H_2O)$ partial pressure ratio.

For the M-edge, no $[Z-y]$ surfaces are stable in the pressure range we considered. We can thus conclude that S—O exchange does not occur on the M-edge and that the metallic edge is stable within the entire domain studied. On the other hand, the surface of the S-edge can be partially oxygenated [1-Z] if $H_2S/H_2O < 1$ (Fig. 5). The surface will be fully oxygenated [4-Z] for $H_2S/H_2O < 0.025$, which means $H_2O/H_2S > 40$ (Fig. 6). These results show that it is essential to keep a partial pressure in H_2S during the HDO process in order to avoid the desulfurization of the catalyst and to maintain the catalytic activity [32].

4. Furan adsorption

The study of furan adsorption has been divided in three parts. The first part deals with the adsorption on the metallic edge, the second part concerns the
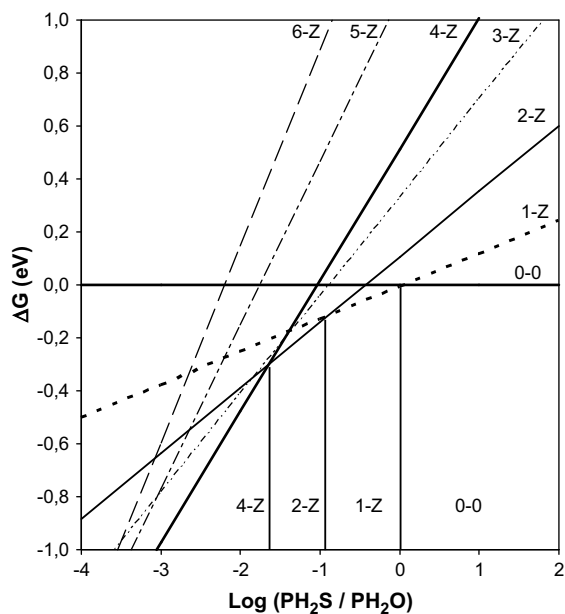
Fig. 4. Sulfur edge: variation of the Gibbs free energy versuslog$((P(H_2S))/(P(H_2O)))$.

non-exchanged sulfur edge, while the third part studies the adsorption on the fully oxygenated sulfur edge i.e. the [4-Z] surface. The adsorption on the stable surface and on coordinatively unsaturated sites (CUS), created by reaction with hydrogen under reductive conditions, was considered. All through this work, a positive adsorption energy corresponds to an exothermic process.

4.1. Adsorption on the metallic edge

Whatever the tested starting geometries, the furan does not adsorb on the metallic edge. The molecule is always desorbed, without any activation barrier, during the geometry optimization.

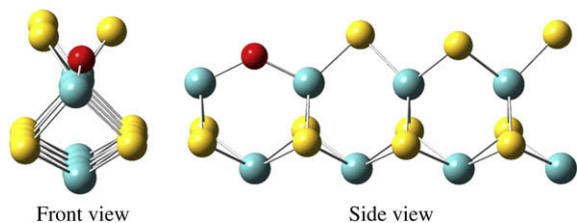It is generally assumed that HDS, HDN and HDO reactions proceed on the CUS of the MoS_2 edges.

Fig. 5. S-edge of [1-Z] surface: stable when $0.01 < H_2S/H_2O < 1$. Molybdenum atoms are in blue, sulfur atoms are in yellow, oxygen atoms are in red.

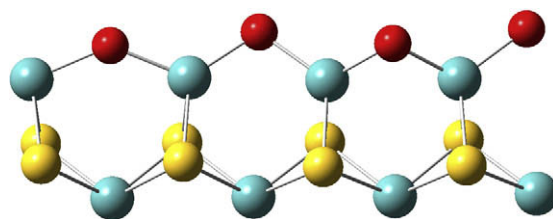Fig. 6. S-edge of [4-Z] surface: stable when $H_2S/H_2O < 0.025$, which means high water partial pressure.

Hence, we also considered the adsorption on vacancies generated by removing one sulfur atom from the edge stable under reducing conditions. This vacancy formation is an endothermic reaction. On the metallic edge, because of the surface reconstruction [15,27,29], two types of vacancies can be created (Fig. 7), yielding two five-fold-coordinated Mo atoms (Mo_{5c}). The most stable defective surface exhibits a ''long'' vacancy (denoted by L hereinafter) created by removing a sulfur atom originally above the long Mo−Mo distance, initially 3.5 Å and 3.6 Å after optimization ($\Delta_r E = 0.54$ eV). The formation of a ''short'' vacancy (denoted by S hereinafter) between the two closer Mo atoms (initially 2.8 Å and 3,2 Å after optimization) is 0.25 eV more endothermic ($\Delta_r E = 0.79$ eV). The η_1 adsorption is possible on both vacancies (Fig. 8), with the oxygen atom of the molecule located in a bridging position between the two Mo_{5c} atoms, and leads to the same geometry. The adsorption energy depends on the type of vacancy: its energy is 0.04 eV for the L vacancy and 0.29 eV for the S vacancy. The global process is endothermic and needs the same energy (0.50 eV) on both vacancies as the final geometries are the same.

To check the affinity of the Mo_{5c} for an oxygen atom that already forms two bonds, we computed the H_2O adsorption energies on these two vacancies. We also calculated the H_2S adsorption energies in order to evaluate the competition effect. The results, reported in Table 2, show that the adsorptions of H_2O and H_2S on both vacancies compete with furan adsorption. Concerning the L vacancy, the adsorption energy of H_2O is higher than the H_2S one. In contrast, these energies are similar on the S vacancy. These findings may be related to the Mo−SH_2 bond (2.55 Å) length which is slightly larger than the Mo−OH_2 one (2.50 Å).

A flat adsorption on the metallic edge with one vacancy is possible (Fig. 9). This η_5 adsorption is endothermic ($E_{ads} = -0.85$ eV) on the L vacancy and requires an important surface reconstruction; one S atom is displaced and located on top of one Mo atom,
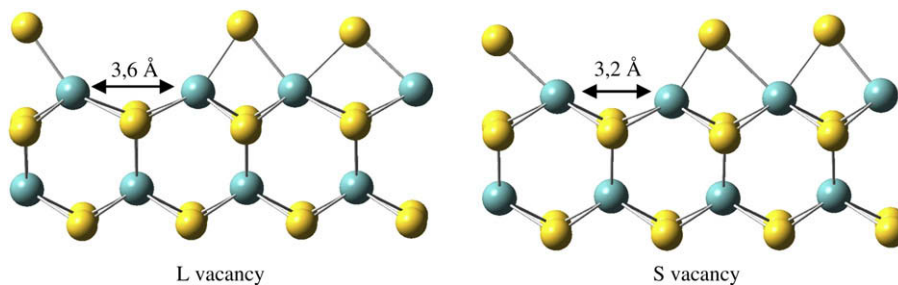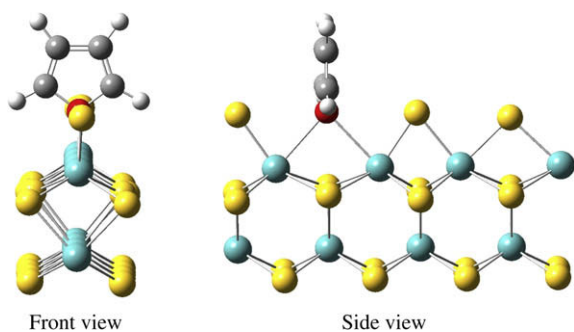
Fig. 7. L and S vacancies located on the M-edge.

forming one S−S bond with its neighbor. The energetic cost of this reconstruction is very high (1.83 eV), hence this kind of adsorption should not occur.

4.2. Adsorption on the reference sulfur edge

Whatever the starting geometries, the furan does not adsorb on the sulfur edge. This is quite surprising since thiophene can adsorb directly on this edge (Table 3) [18]. The average molybdenum−oxygen distance is shorter than the molybdenum−sulfur one. The distance between the furan and the edge would be shorter than the thiophene one, which increase the steric repulsion between the molecule and the edge. The adsorption on the stable edge is not possible and therefore the creation of a CUS is required for the adsorption of furan on this edge.

The vacancy formation by removal of one S atom is more endothermic ($\Delta_r E = 1.61$ eV) on the sulfur edge than on the molybdenum edge. This value is so high that the creation of such CUS should be very limited during the catalytic reaction. On this vacancy, the adsorption energy is slightly exothermic ($E_{ads} = 0.26$ eV). Flat adsorptions are not possible on this edge.

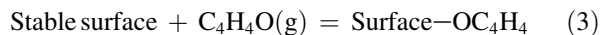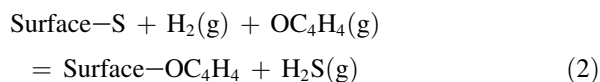### 4.3. Adsorption on the fully oxygenated sulfur edge

Whatever the starting geometry, no minimum has been found for furan or thiophene adsorbed on the fully oxygenated sulfur edge. Once again, a CUS would be required to allow adsorption of molecules on this edge. The creation of such a CUS is even more endothermic ($\Delta_r E = 1.98$ eV) on this edge than on the reference sulfur edge. This value is so high that the creation of such CUS should not occur during the catalytic reaction. We thus assume that this kind of edge cannot be reactive for the furan HDO.

4.4. Discussion

To compare the adsorption on the defective and stable surfaces, the whole process must be considered. The adsorption on defective surfaces must take into account the vacancy formation according to reaction (2), while reaction (3) describes the adsorption of furan on the stable surfaces:

$$\text{Surface−S} + \text{H}_2(\text{g}) + \text{OC}_4\text{H}_4(\text{g})$$
$$= \text{Surface−OC}_4\text{H}_4 + \text{H}_2\text{S}(\text{g}) \qquad (2)$$

$$\text{Stable surface} + \text{C}_4\text{H}_4\text{O}(\text{g}) = \text{Surface−OC}_4\text{H}_4 \qquad (3)$$

The energies of the various reactions involved in the adsorption on the two types of surfaces are summarized in Table 4. Under reductive conditions corresponding to the reaction conditions, the most probable adsorption mode is η_1 on a CUS located on the M-

Fig. 8. Furan adsorbed (η_1) on an L vacancy located on the M-edge.

Table 2
Adsorption energies (eV) for different molecules on CUS located on the M-edge.

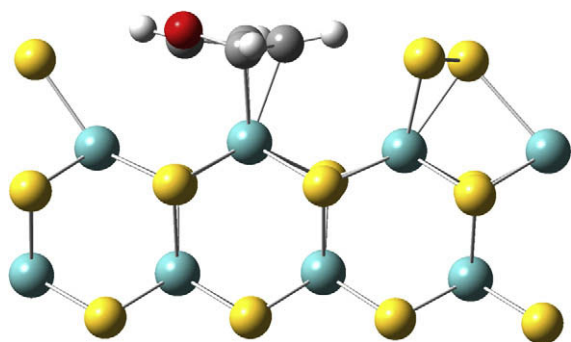| Vacancy	Furan	H$_2$O	H$_2$S	Thiophene
L	0.04	0.47	0.24	0.15
S	0.29	0.10	0.07	−0.04

Fig. 9. Furan adsorbed (η^5) on an L vacancy located on the M-edge.

edge. These results demonstrate that CUS are required for furan adsorption on the edges of the MoS_2 nanoparticles and that the complete adsorption process (vacancy formation plus adsorption) is endothermic. These results are in agreement with experimental data [33] on MoS_2 using radioactive sulfur. The introduction of dibenzofuran in the reactor leads to the departure of sulfur atoms, which is a strong evidence of vacancy formation.

On the other hand, thiophene can adsorb on the non-defective sulfur edge. Therefore, the furan deoxygenation reaction mechanism will be quite different from the thiophene desulfurization and the correlation of thiophene HDS activity with HDO one will not be straightforward.

5. Conclusion

In this work we showed that the stability of the edges of the MoS_2 nanocrystallites depends on the H_2S/H_2O pressure ratio and that the introduction of H_2S in the feedstock is mandatory in order to avoid oxygenation of the catalyst. Furan adsorption on MoS_2 surfaces that is stable under HDO conditions is always endothermic. On defective surfaces, the adsorption is exothermic, but vacancy creation is endothermic and this reaction is activated. The η_1 adsorption on a CUS of the metallic edge is the most favorable adsorption mode and is probably the first step of the reaction mechanism.

Table 3
Adsorption energies (eV) for different molecules on the stable S-edge.

Surface	H_2S/H_2O	Furan	Thiophene
[0-0]	>1	No adsorption	0.18
[4-Z]	<0.025	No adsorption	No adsorption

Table 4
Computed reaction energies (eV) for furan and thiophene adsorption starting from the stable surfaces under reductive conditions.

Edge/surface	Reaction	Adsorption mode	Furan	Thiophene
M/stable surface	(2)	No adsorption		
M/defective surface	(3)	η_1	0.50	0.38
M/defective surface	(3)	η_5	1.39	1.08
S/stable surface	(2)	η_1	No adsorption	0.18
S/defective surface	(3)	η_1	1.35	0.73

References

[1] The Promotion of the Use of Biofuels or Related Other Renewable Fuels for Transport, EU Directive 2001/0265(COD), 25 February 2003.
[2] (a) A.V. Bridgwater, G.V.C. Peacocke, Sustainable Energy Rev. 4 (2000) 1;
(b) G.X. Huber, S. Iborra, A. Corma, Chem. Rev. 106 (2006) 4044.
[3] E. Furimsky, Appl. Catal. A: Gen. 199 (2000) 147.
[4] S. Czernik, A.V. Bridgwater, Energy Fuels 18 (2004) 590.
[5] H. Topsøe, B.S. Clausen, F.E. Massoth, Hydrotreating Catalysts: Science and Technology, Springer, Germany, 1996, pp. 22, 141–144.
[6] E. Furimsky, Appl. Catal. 6 (1983) 159.
[7] O.I. Senol, T.-R. Viljava, A.O.I. Krause, Catal. Today 100 (2005) 331.
[8] A.Y. Bunch, X. Wang, U.S. Ozkan, J. Mol. Cat. A: Chem. 270 (2007) 264.
[9] I.V. Babich, J.A. Moulijn, Fuel 82 (2003) 607.
[10] C. Song, Catal. Today 86 (2003) 211.
[11] S. Brunet, D. Mey, G. Pérot, C. Bouchy, F. Diehl, Appl. Catal. A: Gen. 278 (2005) 143.
[12] M. Sun, J. Adjaye, A.E. Nelson, Appl. Catal., A 263 (2004) 131.
[13] P. Raybaud, Appl. Catal. A. Gen. 322 (2007) 76.
[14] B. Hinnemann, P.G. Moses, J.K. Nørskov, J. Phys.: Condens. Matter 20 (2008) 064236.
[15] J.-F. Paul, S. Cristol, E. Payen, Catal. Today 130 (2008) 139.
[16] S. Kasztelan, H. Toulhoat, J. Grimblot, J.-P. Bonnelle, Appl. Catal. 13 (1984) 17.
[17] P. Raybaud, J. Hafner, G. Kresse, H. Toulhoat, Surf. Sci. 407 (1998) 237.
[18] S. Cristol, J.-F. Paul, C. Schovsbo, E. Veilly, E. Payen, J. Catal. 239 (2006) 145.

[19] G. Kresse, J. Hafner, Phys. Rev. B 47 (1993) 558.
[20] G. Kresse, J. Furthmüller, Comput. Mater. Sci. 6 (1996) 15.
[21] N.D. Mermin, Physiol. Rev. 137 (1965) A1141.
[22] P.E. Blöchl, Phys. Rev. B 50 (1994) 17953.
[23] G. Kresse, J. Joubert, Phys. Rev. B 59 (1999) 1758.
[24] M. Methfessel, A.T. Paxton, Phys. Rev. B 40 (1989) 3616.
[25] J.P. Perdew, A. Zunger, Phys. Rev. B 23 (1981) 5048.
[26] J.P. Perdew, J.A. Chevary, S.H. Vosko, K.A. Jackson, M.R. Pedersen, D.J. Singh, C. Frolais, Phys. Rev. B 46 (1992) 6671.
[27] S. Cristol, J.-F. Paul, E. Payen, D. Bougeard, S. Clemendot, F. Hutschka, J. Phys. Chem. B 104 (2000) 11220.
[28] S. Cristol, J.-F. Paul, E. Payen, D. Bougeard, S. Clemendot, F. Hutschka, J. Phys. Chem. B 106 (2002) 5659.
[29] P. Raybaud, J. Hafner, G. Kresse, S. Kasztelan, H. Toulhoat, J. Catal. 189 (2000) 129.
[30] P.W. Atkins, Physical Chemistry, fifth ed.). Oxford University Press, London, 1990.
[31] D. Loffreda, Surf. Sci. 600 (2006) 2103.
[32] T.-R. Viljava, R.S. Komulainen, A.O.I. Krause, Catal. Today 60 (2000) 83.
[33] T. Kabe, W. Qian, A. Ishihara, J. Phys. Chem. 98 (1994) 912.